MICROBIOLOGICAL METHODS

Cellular Light Scattering for the Identification of Bacteria and Its Application to the Identification of *Staphylococcus*

DAVID L. HAAVIG
Micro Identification Technologies, 970 Calle Amanecer, Suite F, San Clemente, CA 92673
KAYLAGH R. HOLLEN, ABBEY E. DEBRUIN, SHELBI R. LISECKI, and NICOLE C. SHOUP
Northern Michigan University, Biology Department, 1401 Presque Isle Ave, Marquette, MI 49855
MICKEY J.H. STIMAC and ANTHONY M. TRELOAR
Northern Michigan University, Clinical Life Sciences Department, 1401 Presque Isle Ave, Marquette, MI 49855
ZACHARY N. JODOIN, MARGARET S. BOHM, and JOSH S. SHARP
Northern Michigan University, Biology Department, 1401 Presque Isle Ave, Marquette, MI 49855

Rapid identification of bacteria is critical in clinical and food safety applications. This paper describes a novel instrument and data analysis method for identifying bacteria based on the measurement of laser light scattering as the beam interacts with bacterial cells suspended in water. A description of the technology is followed by an identification performance study for a set of strains from the genus *Staphylococcus* (the inclusive target organisms) and a set of non-*Staphylococcus* strains (the exclusive organisms). *Staphylococcus* and non-*Staphylococcus* cells were grown on sheep blood agar (SBA), tryptic soy agar, brain heart infusion (BHI) agar, or Luria–Bertani (LB) agar and identified based on how cells scattered light. Bacteria from the genus *Staphylococcus* grown on solid media were correctly identified more than 92% of the time. To determine whether the system could also identify bacteria grown in liquid culture, six different *Staphylococcus* strains and six different non-*Staphylococcus* strains were grown in tryptic soy broth, BHI broth, or LB broth. This system accurately identified all targeted *Staphylococcus* samples tested, and no misidentifications occurred. A single-blind identification experiment was also performed on human clinical isolates obtained from the Upper Peninsula Health System. Ninety blind-coded clinical bacterial isolates on SBA were tested to determine whether they were from the genus *Staphylococcus*. All *Staphylococcus* were accurately identified, and no misidentifications occurred. This study demonstrated the proof of concept of a novel system that can rapidly and accurately identify bacteria from pure culture based on cellular light-scattering properties.

Received March 9, 2017. Accepted by AH May 17, 2017.
Corresponding author's e-mail: dhaavig@micro-identification.com
Supplemental information is available on the *J. AOAC Int.* Web site, http://aoac.publisher.ingentaconnect.com/content/aoac/jaoac
DOI: 10.5740/jaoacint.17-0097

Rapid identification of bacterial pathogens in clinical specimens has been correlated with improved patient outcomes (1). The faster pathogens are identified, the sooner the appropriate therapy can be administered. From a food safety perspective, rapid identification of pathogens at production facilities can prevent contaminated foods from reaching the public or result in the recall of products to minimize public exposure to disease-causing organisms. The majority of rapid bacterial identification technologies are designed to detect biological material, such as nucleic acid or protein, from specific microorganisms. Here, we describe a novel non-nucleic acid-based technology that uses laser light scattering to identify unlabeled bacterial cells. Previous technologies used light scattering as a means of bacterial identification. However, these technologies measured light scattering off colonies or labeled cells. One such technology evaluates the forward scatter pattern of laser light that passes through a bacterial colony and the solid culture medium on which the bacterium was grown (2). This technology has been successfully used to identify isolated colonies from genera *Listeria* (3) and *Vibrio* (4), *Salmonella enterica* (5), and others on culture plates containing a mixture of species. Comparatively little is known about using light-scattering measurements directly from bacterial cells for identification. Previous work by Koch and Ehrenfeld (6) showed that bacterial size, shape, and volume could be calculated by light-scattering measurements. In 1968, Wyatt (7) proposed that light scattering could be used to identify bacteria because different species of bacteria would have unique light-scattering patterns due to their structural and biochemical differences. Katz et al. (8) demonstrated that bacterial size could be determined by elastic light-scattering measurements in 2003. Using light-scattering measurements to rapidly identify bacteria has been progressing. Jo et al. (9) used Fourier transformations of two-dimensional angle resolved light-scattering maps to identify rod-shaped bacteria. Single cells of *Staphylococcus aureus* that were labeled with conjugated gold nanoparticles were identified by light-scattering technology (10). The length and diameter of single cells of unlabeled *Escherichia coli* were determined by angle-resolved light scattering by a scanning flow cytometer (11). Here, we describe a bacterial identification method capable of processing an unlabeled suspension of cells of the same genus or species in filtered water. This method uses an instrument, a Micro Identification Technologies (MIT) 1000 System (hereafter designated the

MIT 1000), to measure laser light scatter off a sequence of microscopic particles suspended in water. As each particle is measured, the measurement values are simultaneously analyzed by a series of software objects called "Identifiers™." Each Identifier object applies a statistical classification algorithm (12) to the input values to determine whether the collection of particles being measured belongs to the microorganism class (a specific genus or species) the Identifier was designed to classify. Each Identifier analyzes a sufficient number of particles, typically 10–40, for its classification algorithm to converge to a class membership determination. Each final Identifier result is either a (*1*) positive result, indicating that the sequence of measured particles are members of its class; or (*2*) negative result, meaning the measured sequence of particles are not members of its class. The identification of the sample is reported by listing the class of the Identifier with the positive result or, if there are no positive results, the sample is listed as "Unknown."

The MIT 1000 and a *Listeria* genus Identifier were previously validated under the AOAC Research Institute's *Performance Tested Method*^{SM} (PTM) Program (13) and awarded PTM Certificate No. 060901 for the identification of the genus *Listeria* (14); however, a detailed technical description of the system or identification method was not published. In addition to the technical details of the MIT 1000, the development of a *Staphylococcus* genus Identifier to identify bacteria within the genus *Staphylococcus* is also described in this work.

The genus *Staphylococcus* was chosen as a target for identification because it contains a number of significant human and animal pathogens. *S. aureus* is the most common cause of bacterial infections in humans (15, 16). It can cause numerous types of infections, ranging from mild skin infections, such as pimples and boils, to serious tissue abscesses, bone infections, and sepsis. *S. aureus* is also a significant burden in the dairy industry, as it is the leading cause of bovine mastitis and a major reason for antibiotic treatment in cows (17). Additionally, *S. aureus* is an important foodborne pathogen because it can secrete a number of heat-stable enterotoxins into food that can cause the rapid onset of nausea, vomiting, and diarrhea (18). Other species of *Staphylococcus* are important pathogens as well. *S. epidermidis* can cause disease in immunocompromised patients or those who have implanted medical devices, such as artificial joints, catheters, or intravenous lines (19). *S. intermedius* is a zoonotic pathogen that can cause infections in both humans and animals (20). Finally, members of the *Staphylococcus* genus grow in grape-like clusters, whereas the *Streptococcus* genus grows in chains; on the other hand, the *Micrococcus* genus grows in tetrads. These growth arrangements may give these bacteria unique light-scattering patterns that are detectable by the MIT 1000.

This work explores the initial basis of using laser light scattering to identify the genus *Staphylococcus*. The performance testing of this work focused on the ability of the MIT 1000 to distinguish *Staphylococcus* bacteria from bacteria of similar size and shape, such as from genera *Streptococcus* and *Micrococcus*. The ability of the system to distinguish the genus *Staphylococcus* from more diverse bacteria, such as *E. coli*, *Bacillus subtilis*, and *Listeria monocytogenes*, was also examined. Because growth media and growth conditions can potentially alter the size and shape of bacteria, the performance of the system to identify bacteria on several types of solid and liquid media was explored. Ultimately, this system could function as a low-cost rapid bacterial detection method that could have important applications in medical, veterinary, or food safety fields.

Principle of the Method

MIT 1000 Technology

The MIT 1000 instrument is a laser-based, rapid microbial identification (RMID) system capable of identifying bacteria from a pure culture. Inspired by a device developed to detect phytoplankton in seawater (21), the instrument uses the principles of light scattering (22) to identify the genus of bacterial cells that are suspended in filtered water. Measurements of individual cells give optical absorption values of about 1 m^{-1} at optical wavelengths (23, 24). Consequently, given the microscopic size of a cell, visible light does not merely reflect off the cell membrane; it also penetrates the cell membrane with virtually no attenuation and interacts with constituent features within the cell to produce a complex three-dimensional intensity scattering pattern when the light leaves the vicinity of the cell. The MIT 1000 measures this three-dimensional pattern at 35 positions around the cell. As stated above, these resulting light patterns have been shown to contain bacterial genus-specific information (13). To use this information to identify bacteria, light patterns for known strains are collected and analyzed to select the light-scattering features that best discriminate between an inclusive target class (of bacterial genus, species, serotype, or other subtype) and all other exclusive, nontarget bacterial strains. The selected light-scattering features are used to create the Identifiers. Subsequently, the Identifier can analyze light-scattering measurements of an unknown pure genus or species bacterial suspension to determine whether the unknown cells belong to its target bacterial class.

System Design

The MIT 1000 System consists of a rigid optical platform with five concentric arcs of photodetectors, with eight detectors on four of the arcs and three on the fifth (bottom) arc (Figure 1). Through detector ports in the arcs, the detectors view the center of curvature. The beam of a horizontally polarized red 660 nm solid-state laser with a Gaussian beam profile also passes through the center of curvature. Finally, the round section of a 15 mL round-bottomed flask, called the "MIT 1000 Sample Vial," is positioned concentric with the arcs. Four arcs are positioned to form a letter "X," with 90° between adjacent arcs as viewed along the laser beam path. Each of these arcs hosts eight

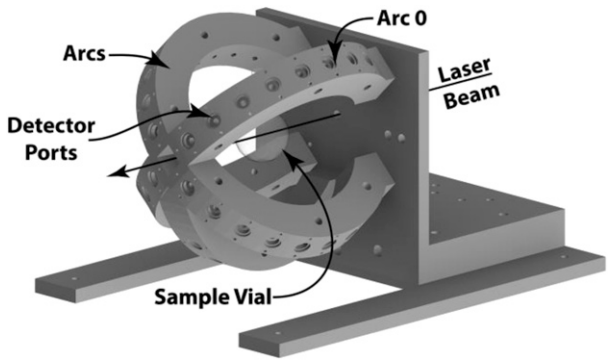

Figure 1. The optical platform of the MIT 1000 System.

photodetectors. The remaining arc is located at the bottom, positioned between the two lower arcs of the X and hosts three photodetectors. The arcs are numbered 0 through 4 clockwise, starting with the upper right-hand arc when facing into the laser. The eight photodetectors mounted along the arcs are spaced every 15°, starting at 15° from the forward-scattering end. The detectors on each arc are numbered 0 through 7, in which detector 0 corresponds to the detector at 15° and detector 7 is the detector at 120°. Arc 2, the lowest arc, has detectors mounted at 45, 60, and 120°. It also provides a bottom support for the sample vial. Each detector in the system is referenced by its arc–angle coordinate, such as detector 1–2, which is the third detector (at 45°) on arc 1. The detectors are also referred to by their system index value beginning with detector 0–0 having system index 0 and ending with detector 4–7 having system index 34: Detectors with system index 0–7 are on arc 0, 8–15 are on arc 1, 16–18 are on arc 2, 19–26 are on arc 3, and 27–34 are on arc 4, in which the lowest index on each arc (except for arc 2) corresponds to the photodetector mounted at 15° from forward scatter. All photodetectors are mounted to view the center of curvature of the arcs, and, therefore, the center of the sample vial through a 2.5 mm diameter hole along the radius of the 2.5 cm thick arcs. The field of view of the photodetectors is about 5°, and the 2.5 mm diameter active area of the photodetector subtends an angle of about 1.5°, as viewed from the arc center of curvature. The Gaussian beam of the laser has a 0.1 mm diameter beam waist and is positioned so that the axial center of the beam waist is also at the center of curvature of the arcs. The beam direction is shown in Figure 1. Although particles in the sample vial can pass through the laser beam at any position along the beam path, because of their limited field of view, the photodetectors will only measure those particles passing through the laser beam near the center of curvature of the arcs. The detectors, which have no light-polarization sensitivity, are calibrated to measure a value proportional to watts of incident power measured from a 1 mm diameter Lambertian source-emitting red light with a spectral bandwidth of ±11 nm centered at 660 nm. When the calibration is applied to the detector measurement, the resulting values are proportional to the irradiance (W/cm^2) of the light incident on the detector and are also proportional to the radiant intensity (W/sr, where sr = steradian) of point light sources.

Particle Measurements in the MIT 1000

A particle-scattering measurement (i.e., an event) is measured in volts (vertical axis) versus time in seconds (horizontal axis) as the particle passes through the laser beam, as shown in Figure 2. This plot shows the measured scattering signal for one 1.6 µm diameter polystyrene sphere versus time in seconds. The curves are plots of the measured raw voltage signal from three of the detectors on arc 1. The measured signal depends on the size, shape, and optical properties of the particle and where in the Gaussian cross section of the beam the particle was located. The polystyrene sphere plots exhibit a Gaussian curve profile because the intensity profile of the laser is Gaussian and the particle is spherically symmetric and homogeneous.

Mie (25) developed a mathematical prediction of light scattering off isolated small spherical particles like the polystyrene latex spheres used here. This Mie prediction has been implemented in a number of ways, including algorithms (22) and online calculators (26), to predict

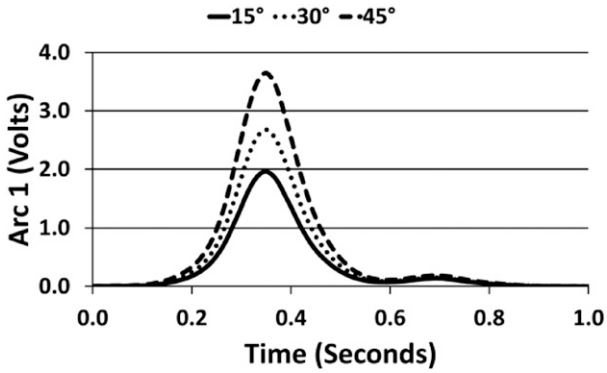

Figure 2. A representative measured signal from the three detectors on arc 1 of one 1.6 µm diameter polystyrene sphere. The angle indicates the position of the photodetector on the arc.

scattering intensity versus angle for spheres, such as those described in Figure 2. In Figure 3, the Mie prediction, using the input parameters given in Table 1 for each of the eight detector positions on arc 1 for the event described in Figure 2, is shown normalized to a Mie-predicted scattering intensity of 1.0 at 0°. Also shown are the actual scaled measured intensity values after calibration for all eight detectors at the time when the signal from the detector at 15° attained its maximum value (at about 0.35 s). The calibrated measurements from each detector were scaled by a factor such that the value for the detector at 15° matched the Mie prediction at 15°. Figure 3 shows good agreement of the scaled calibrated measured values with the Mie prediction.

Figure 4 shows an event of *S. aureus* [American Tissue Culture Collection (ATCC), Manassas, VA 9144; *S. aureus* 9144]. The data shown in Figure 4 are from the same arc used in Figure 2. Because the size and shape of *S. aureus* 9144 vary from individual cell to individual cell and because individual *Staphylococcus* cells may stick together, the event plots show significant deviations from a Gaussian profile. Because orientations of the particles are not constrained as the measurement is made, measurements of distinct particles or even remeasurement of the same particle will produce distinctly different event profiles.

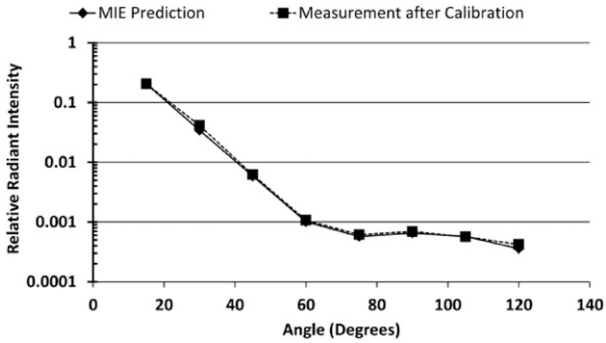

Figure 3. Comparison of a Mie prediction and the calibrated results from the data shown in Figure 2. The Mie prediction input parameters are presented in Table 1. The Mie prediction was scaled to a value of 1 at 0°. The values of the calibrated measurements were taken at the time when the 15° detector reached its maximum value (at about 0.35 s). All values were then scaled by a factor such that the value for the 15° detector equaled the Mie prediction at 15°.

Table 1. MIE prediction input parameters

Parameter	Value
Sphere diameter	1.59 μm
Sphere index of refraction	1.585 (37)
Water index of refraction at 25°C	1.331
Incident light wavelength	660 nm

Identification Algorithm

The variability of cell size and shape, angular orientation, location, and chemical makeup of the features and structures inside and outside the cell make analytical and numerical prediction of scattering radiant power a complex task. Because the Mie solution applies only to spheres, MIT developed a statistical classification algorithm (12) that classifies the light-scattering measurements made by the MIT 1000 System, such as those in Figures 2 and 4. When microbes like bacteria are measured, the classification is identification to the desired bacterial taxonomic level (e.g., genus, species, etc.) The details of the algorithm are proprietary to Micro Identification Technologies and will not be fully exposed here, but the general principles are described. The algorithm is based on a normalized frequency of occurrence histograms taken from a large set of calibrated measurements of bacterial samples. These normalized histograms are used as probability densities, which, when combined with measurements of new or unknown bacterial cells, produce probabilities of bacterial identification.

The concept of the identification process can be demonstrated with a polystyrene sphere and *S. aureus* 9144 measurements, as shown in Figures 2 and 4. Scattering measurements, like those in Figures 2 and 4, contain a large quantity of raw data. Additionally, varying event durations, cell feature variations—such as cell shape, the possible presence of flagella (possibly moving), and the possibility that multiple cells may stick together—result in light-scatter plots that significantly vary from one measured particle to the next, even when the cells are of the same bacterial strain. One cannot simply look at scattering measurements of bacterial cells, such as the one shown in Figure 4, to determine whether it is from one bacterial strain or another. The MIT 1000 implements a procedure that ensures that values taken from the measurement of one particle can always be correlated to the measurement of any other cell. This procedure is illustrated in Figure 5 using the event shown in Figure 2. The vertical line labeled T_r is positioned at the time detector, D_r, and attains its maximum value. The variable r is the system index of the detector. The time, T_r, can be determined in all measured events. Once this time is set, values from all detectors are taken. Figure 5 shows an example for values v_{ir} and v_{jr} taken from two detectors, D_i and D_j, at time T_r. Doing this for all detectors results in a set of 35 values, v_{1r} through v_{35r}, each taken from the event at the time specified by T_r. At this point, the detector calibrations are applied to each of these raw voltage values, resulting in the calibrated values R_{1r} through R_{35r}. This set of calibrated values is called a "Time Set." Another Time Set of 35 values can be taken from the same event measurement by selecting a different detector, system index s, to specify the time T_s by identifying when detector D_s is at maximum value and taking the values of all detectors at that time. This yields, after calibration, the time set R_{1s} through R_{35s}. Repeating this for all 35 detectors produces 35 Time Sets. Each value, R_{ij}, is called a "Descriptor." Importantly, this procedure to generate Descriptors can be applied to every event measurement.

Each measurement of a polystyrene sphere will result in a set of Descriptors unique to that sphere due to the variation in sphere sizes and material properties. This variation in the Descriptors is easily demonstrated by creating frequency-of-occurrence histograms from the Descriptors. Furthermore, it is convenient to use ratios of Descriptors to minimize time dependencies in the laser output and possible slow electronic signal drift. The analysis below uses two-dimensional histograms with each histogram using four Descriptor values from the same Time Set, T_j: R_{aj}, R_{bj}, R_{cj}, and R_{dj}. The horizontal (x) and vertical (y) positions on the two-dimensional histogram for each class of particle are calculated from simple functional relationships between Descriptors, such as

$$x = \frac{R_{aj}}{R_{bj}}$$

and

$$y = \frac{R_{cj}}{R_{dj}}$$

This selection of a Time Set plus the definition of x and y from the four Descriptor values is called a "Discriminant Function." Figure 6a shows one such histogram for about 200 000

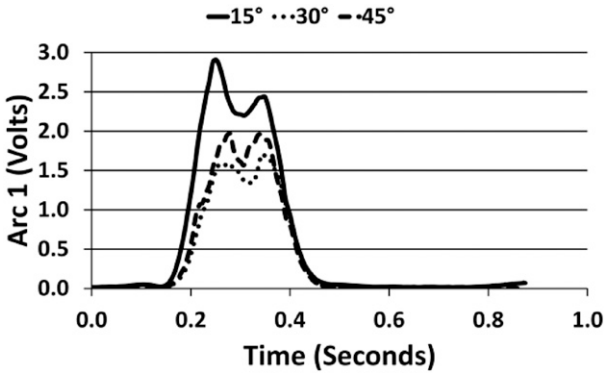

Figure 4. Measured signal from the three detectors on arc 1 for *S. aureus* (ATCC 9144). The angle indicates the position of the photodetector on the arc.

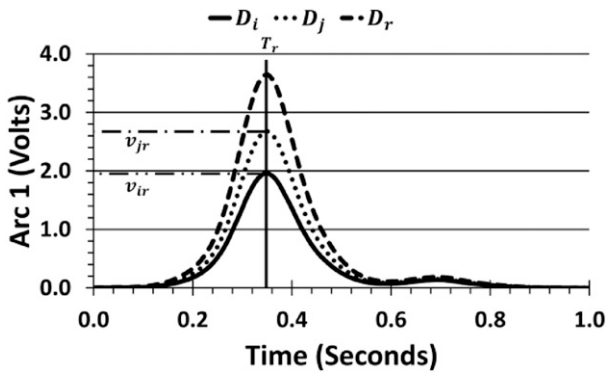

Figure 5. Values v_{ir} and v_{jr} were derived from the measurement of detectors D_i and D_j at time T_r, when the signal from detector D_r was at maximum value.

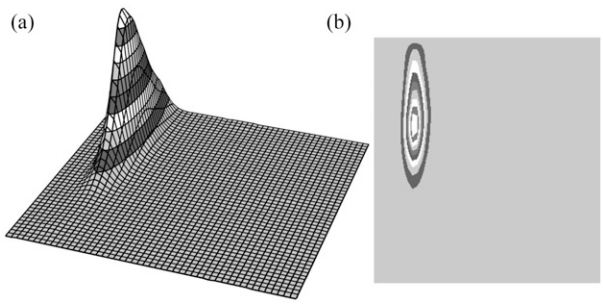

Figure 6. (a) Histogram and (b) contour plot in arbitrary units for approximately 200 000 events of polystyrene spheres using the discriminant function 3:1,11,19,3. Both axes are in dimensionless units derived from the ratio of two radiance values.

polystyrene spheres for the Discriminant Function, $j = 3$, which is T_3 defined by D_3; and $a = 1$, $b = 11$, $c = 19$, and $d = 3$, which is written as 3:1,11,19,3. When a height-dependent shading scheme is used on the histogram, as shown in Figure 6a, and viewed from above, it appears as the contour shown in Figure 6b, in which the shaded bands correspond to the height of the original histogram. The contour graphically shows the full range of possible values of x and y derived from all measured 1.6 μm diameter polystyrene spheres for the Discriminant Function 3:1,11,19,3.

Because the size and shape of the contour result from small differences in the size, shape, and material properties of the spherical particles, it is expected that performing the same analysis on a different type of particle will produce contours that are different from those of a sphere. Figure 7 shows contour plots from about 200 000 events for 11 bacterial strains using the same Discriminant Function and the same axes scale and limits used in Figure 6. Additionally, the crosshair has the same coordinates in each contour. Finally, Figure 7a is the same contour shown in Figure 6b, for comparison.

Figure 7g shows the contour for *S. aureus* 9144. There is virtually no overlap in the two contours of Figures 7a and g. If an experiment were performed in which either one 1.6 μm diameter polystyrene sphere or one *S. aureus* 9144 cell were selected at random and then measured by the MIT 1000 System, the identity of the unknown particle could be revealed by determining the x and y values for the unknown using the Discriminant Function as defined above and plotting that coordinate on Figure 7a and g. If the coordinate is within the sphere's contour, then the unknown is highly likely a 1.6 μm diameter polystyrene sphere. Likewise, if it is within the contour of *S. aureus* 9144, then it is highly likely an *S. aureus* 9144 cell. If the coordinate is not within either contour, then the identity of the unknown cannot be determined.

Clearly, it is easier to distinguish the contour plot of the sphere from any of the 11 bacterial strains than distinguishing between the bacterial strains. It is evident from Figure 7, however, that the size, shape, and location of the contours do show a species and even strain dependence—a dependence that may be used to identify bacterial species.

Normalizing the frequency of occurrence histograms allows us to interpret them as a probability density (27), namely $f(x, y)$. This set of probability distributions can now be used with a Bayesian decision theory (28) approach to try to identify unknowns. In its simplest form, the descriptor values would be taken from the measurement of a single event of the unknown

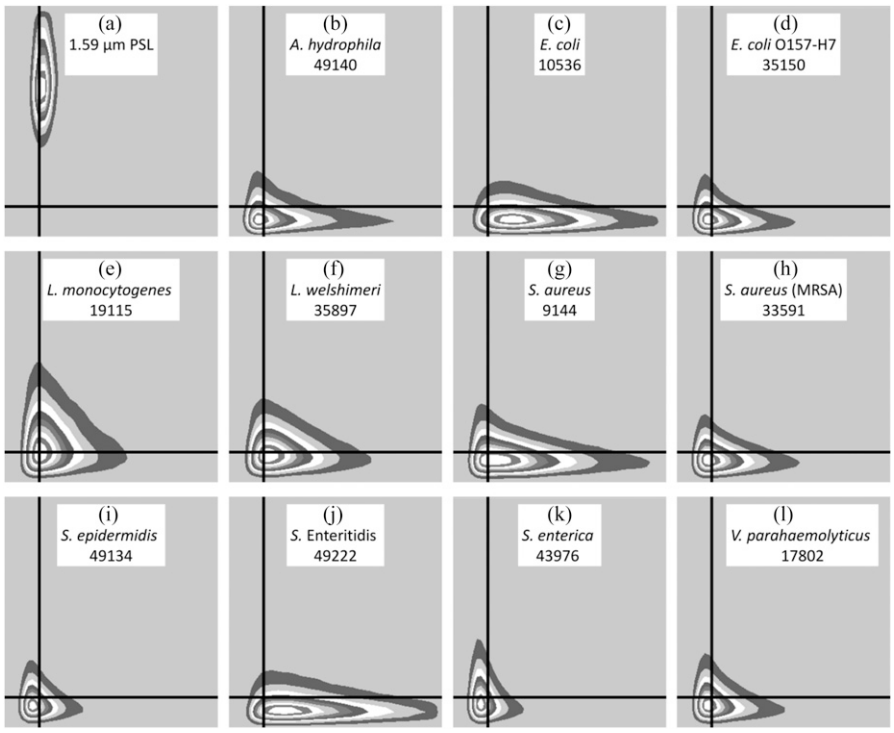

Figure 7. Contour plot of polystyrene spheres (a) compared with the contour plots of 11 bacterial strains (b–l). Each plot is derived from ~200 000 events and all used the same discriminant function, 3:1,11,19,3. The plots have the same *x*- and *y*-axis limits used in Figures 5–7. Bacterial strains shown are as follows: (b) *Aeromonas hydrophila* ATCC 49140, (c) *E. coli* ATCC 10536, (d) *E. coli* ATCC 35150, (e) *L. monocytogenes* ATCC 19115, (f) *L. welshimeri* ATCC 35897, (g) *S. aureus* ATCC 9144, (h) *S. aureus* ATCC 33591, (i) *S. epidermidis* ATCC 49134, (j) *S. enterica* subsp. *enterica* serovar *Enteritidis* ATCC 49222, (k) *S. enterica* subsp. *indica* ATCC 43976, and (l) *V. parahaemolyticus* ATCC 17802.

bacterial species and the Discriminant Function values of x and y calculated. The presumptive identification of the unknown is the bacterial species with the highest value of probability density at the coordinate x,y. Although the probability densities are different, the difference is small, and this simplistic analysis would lead to many inaccurate identifications. A better approach is to calculate, for each bacterial species in the set, the probability that the unknown is that species:

$$\{P_1\} = \{f_1(x_1, y_1)\}$$

where $\{f_1(x_1, y_1)\}$ = set of probabilities for each species and the index "1" = Discriminant Function used to create the densities. Although this, by itself, is not an improvement, the probability set, $\{P_1\}$, can be combined with a second set of probabilities, $\{P_2\}$, from a second Discriminant Function (index 2), using standard methods (29). Both $\{P_1\}$ and $\{P_2\}$ are derived from the measurement of one cell. This combined probability gives an improved identification probability. Again, the simple interpretation is that the presumptive identification is the species associated with the highest probability after the calculation. The combined probability distribution is easily improved again by using additional probability sets from other Discriminant Functions. As more probability sets are combined, the resulting probabilities converge to fixed values, $\{P\}_{event}$. When the simple interpretation is used on this converged set of probability values, testing shows that the presumptive identification based on the species associated with the highest probability is correct 60–85% of the time, depending on the actual species of the cell.

Additional discriminating information is still needed before a definitive identification can be made. The identification process is significantly enhanced if multiple cells of the same unknown species are measured. As described above, after measuring the first event, a calculated set of probabilities is created: $\{P\}_{event\ 1}$. A second measured event produces a second completely independent set of probabilities: $\{P\}_{event\ 2}$. Combining the identification probabilities for these two measurements produces another improved estimate in the identification of the species of the unknown: $\{P\}_{1-2}$, where "1–2" = "events 1 through 2." A third measured event produces a third set of probabilities, which, when combined with $\{P\}_{event\ 1}$ and $\{P\}_{event\ 2}$, gives an even better estimate: $\{P\}_{1-3}$.

Figure 8 illustrates an example of the process for a stream of unknown cells, each of the same strain. This graph shows the plot of $\{P\}_{1-i}$ versus event i, in which i is the index of the event that was measured. As more events are measured and processed, the probability for *E. coli* O157:H7 gets closer to 1 (100%) and all other probabilities drop toward zero (0%). This process of analyzing additional events is continued until the highest probability passes a predefined confidence criterion, such as the probability of the most likely species is greater than 0.999 for five event analyses in a row, as shown. Then the stream of unknown cells is identified as the one genus, species, or strain that has a probability of very near 1: In this case, the identification is *E. coli* O157:H7.

This collection of probability distributions provides quick and accurate identification of any of the species that are in the set of probabilities. For the collection that was used to create Figure 8, the algorithm essentially asks the question of the data stream, "Is this data stream consistent with a stream of one of the strains of *E. faecalis* or *E. coli* O157:H7 or *E. coli*, or genus *Salmonella* or *S. aureus* or *S. epidermidis* cells?" However, this is a closed process. If the stream of unknown cells does not belong to one of the species in the set of probabilities—for example, if the unknown cells are *V. parahaemolyticus*—the results of the test are unpredictable. To avoid these unpredictable results, the proprietary Micro Identification Technologies algorithm uses the same probability densities described above to create an open equivalent to this closed collection of probability densities. This new, refined collection of probability densities is called "Identifier." The Identifier has a similar interpretation to the collection described above but contains only two classes of probability densities and associated bacterial species: (*1*) the target taxonomic group and (*2*) all other types of bacteria.

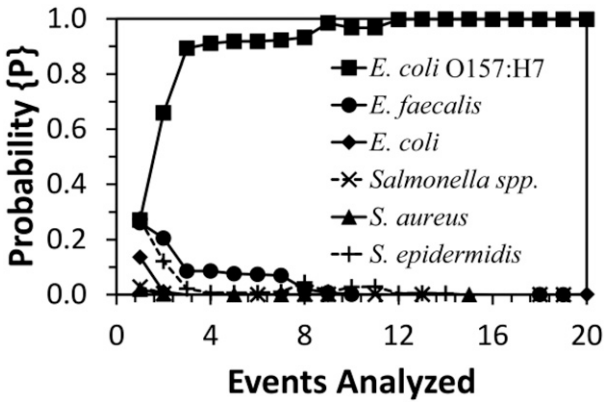

Figure 8. Plots showing the convergence of identification probabilities as a function of the number of events analyzed. As additional cells of the unknown sample are measured, the probability line of *E. coli* O157:H7 approaches 1 (100%) and all others approach zero (0%). The MIT 1000 identified the sample as *E. coli* O157:H7 after measuring and analyzing 20 cells (events).

Identifiers are constructed from a collection of bacterial strains that are members of the target taxonomic group (i.e., the target strains) and strains that are not members of the target group (i.e., the converse strains). Creating a stream of bacterial cells of the same species is a simple and rapid process when using colonies of bacteria grown on solid agar plates. In nearly all circumstances, all bacterial cells in a single isolated colony grown on agar plates are of the same genus and species, and the prepared sample vial contains several thousand cells per cubic centimeter. An Identifier designed to identify the genus *Listeria* asks the question of the data stream, "Is the data stream consistent with the genus *Listeria*?" The resulting answer is now either, "Yes, it is consistent with the genus *Listeria*" or "No, it is not." A stream of bacterial cells that are not members of the *Listeria* genus will result in a No answer. The genus *Listeria* Identifier will allow the MIT System to determine whether a stream of the same strain of bacterial cells is or is not from the genus *Listeria*. Likewise, the *E. coli* Identifier allows the MIT System to determine if the stream is or is not *E. coli*. The Identifiers operate independently and can be used simultaneously. For example, when simultaneously using the genus *Listeria* and *E. coli* Identifiers, the MIT 1000 can determine whether the test sample is from the genus *Listeria*, *E. coli*, or neither, in one test.

Experimental

Apparatus

(**a**) *MIT 1000 System.*—Micro Identification Technologies.

(**b**) *Desktop computer with MIT RMID software*.—Micro Identification Technologies.

(**c**) *Organism library license.*—Full-time access to all MIT Identifiers, Micro Identification Technologies.

(**d**) *RMID Sample Vial.*—Part No. 20007, Micro Identification Technologies.

(**e**) *RMID Sample Vial holder.*—Part No. 10011, Micro Identification Technologies.

(**f**) *Pipets.*—Capable of delivering 1 and 200 µL.

(**g**) *Microcentrifuge*.

(**h**) *Vortex mixer*.

Reagents

(**a**) *Filtered water.*—Prepared using a three-stage water filter with a sediment filter, precarbon filter, and a 0.2 µm ultrafilter filter, WQCFU-T-KIT, Watts Water Technologies (North Andover, MA).

(**b**) *Tryptic soy agar (TSA).*—G62, Hardy Diagnostics (Santa Maria, CA).

(**c**) *Sheep blood agar (SBA).* —A10, Hardy Diagnostics.

(**d**) *Brain heart infusion (BHI) agar*.—C5121, Criterion

(**e**) *Luria–Bertani (LB) agar.*—C6001, Hardy Diagnostics.

(**f**) *Tryptic soy broth (TSB).*—U65, Hardy Diagnostics.

(**g**) *BHI broth.*—C5141, Criterion.

(**h**) *LB broth.*—U35, Hardy Diagnostics.

Procedure

(**a**) *Sample preparation from agar culture.*—(*1*) Transfer one isolated colony to 200 µL filtered water in a 500 µL microcentrifuge tube using a sterile 1 µL plastic inoculating loop.

(*2*) Mix on a vortex mixer for 20 s.

(*3*) Transfer 1–5 µL suspension to an MIT Sample Vial containing 20 mL filtered water and seal with parafilm.

(*4*) Tip the sample vial and place it into the MIT 1000.

(**b**) *Sample preparation from liquid culture.*—(*1*) Transfer 100 µL broth culture to a microcentrifuge tube and centrifuge at 4000 × *g* for 4 min.

(*2*) Remove the supernatant broth.

(*3*) Add 500 µL filtered water, mix on the vortex mixer, and centrifuge at 4000 × *g* for 4 min.

(*4*) Remove the supernatant liquid.

(*5*) Resuspend the cell pellet in 1250 µL filtered water by mixing on the vortex mixer for 20 s.

(*6*) Transfer 0.5 µL final bacterial cell suspension into the MIT Sample Vial containing 20 mL filtered water and seal with parafilm.

(*7*) Tip the sample vial and place it into the MIT 1000.

(**c**) *Analysis.*—Press the "Identify" button in the MIT 1000 User Interface Program. The identification test measures 10–40 events, taking from 30 s to 5 min to complete each test depending on the sample vial concentration. The average test time is 2 min. The results are displayed on the MIT 1000 User Interface and recorded. The Identification test result is either an identification of the sample as given by one or more Identifiers in use, or the result is "Unknown," meaning the measured sample was not found to match any of the Identifiers in use.

Staphylococcus Species Identifier Development

To construct the genus *Staphylococcus* Identifier, the target and converse strains listed in Table 2 were streaked for isolation and grown on TSA at 37 ± 2°C for 18 ± 2 h (30,31,32). The target strains included seven strains of *S. aureus*, one strain of *S. capitis*, two strains of *S. epidermidis*, two strains of *S. lugdunensis*, one strain of *S. schleiferi*, two strains of *S. sciuri*, and two strains of *S. warneri*. The converse strains were composed of three species, including four strains of *E. coli*, one strain of *Proteus mirabilis*, and five serovars, including two subspecies of *S. enterica*. The aim was to construct an initial Identifier that would detect a number of different *Staphylococcus* spp. By using only the strains listed in Table 2, it is possible that the resulting Identifier is not inclusive of all known *Staphylococcus* spp. Limited testing was performed on other *Staphylococcus* spp. that were not *S. aureus*, *S. epidermidis*, or *S. intermedius*. *See* Figure S1 for the identification test results of *S. haemolyticus*, *S. chromogenes*, and *S. xylosus* grown on blood gar. Each of these strains was correctly identified as belonging to the genus *Staphylococcus*.

Samples of each target and converse strain were prepared according to the method described above for sample preparation from agar culture. Each sample vial was measured once for 1 h, collecting measurements of approximately 1000 individual particles. Additional sample vials were made and measured until a total number of about 200 000 events were measured for each target and converse strain. These measurements were used to form histograms and/or probability densities and were analyzed as described above. The Identifier was then constructed from a collection of probabilities chosen and assembled by a method proprietary to MIT. If a strain was identified as belonging to the genus *Staphylococcus*, the MIT 1000 would display the identification as a *Staphylococcus* sp.

Staphylococcus Species Identifier Performance Testing

The performance of the genus *Staphylococcus* Identifier was evaluated by performing identification tests on known bacterial strains grown on solid or liquid media. In addition, a single-blind identification experiment was performed on human clinical isolates obtained from the Upper Peninsula (UP) Health System in Marquette, MI. The samples were prepared and identified using the following methods:

(**a**) *Solid media identification performance testing.*—The bacterial strains listed in Table 3, except for *B. subtilis*, were grown for 18 ± 2 h at 37 ± 2°C on SBA, LB agar, TSA, or BHI agar. Samples were then prepared as described in the procedure above. Each strain was measured in the MIT 1000 a minimum of 10 times using independent colonies for analysis.

(**b**) *Liquid media identification performance testing.*—A select number of strains, listed in Table 3, were grown for 18 ± 2 h at 37 ± 2°C on SBA. For each strain, one isolated colony was used to inoculate 2 mL TSB, 2 mL BHI broth, or 2 mL LB broth. The broth tubes were shaken at 200 rpm for 18 ± 2 h at 37 ± 2°C. Following incubation, the samples were prepared according to the procedure above. The wash step was performed to remove any undissolved particulate matter present in the growth media that might interfere with the identification

Table 2. Target and converse bacterial strains used to construct the genus *Staphylococcus* Identifier[a]

Organism	Source and strain	Origin
Target bacterial strains		
Staphylococcus aureus subsp. *aureus*	ATCC 6538	Human lesion
Staphylococcus aureus subsp. *aureus*	ATCC 9144	Unknown
Staphylococcus aureus subsp. *aureus*	ATCC 25923	Clinical isolate
Staphylococcus aureus subsp. *aureus*	ATCC 29737	Unknown
Staphylococcus aureus subsp. *aureus*	ATCC 33591	Unknown
Staphylococcus aureus subsp. *aureus*	ATCC 700698	Human sputum
Staphylococcus aureus subsp. *aureus*	NRRL B-1448[b]	Food poisoning
Staphylococcus aureus subsp. *ureolyticus*	ATCC 49325	Human inguinal area
Staphylococcus epidermidis	ATCC 49134	Clinical isolate
Staphylococcus epidermidis	ATCC 49461	Clinical isolate
Staphylococcus lugdunensis	ATCC 43808	Axillary lymph node
Staphylococcus lugdunensis	ATCC 700328	Unknown
Staphylococcus schleiferi subsp. *schleiferi*	ATCC 43808	Jugular catheter
Staphylococcus sciuri subsp. *sciuri*	ATCC 29061	Southern flying squirrel skin
Staphylococcus sciuri subsp. *sciuri*	ATCC 29062	Eastern flying squirrel skin
Staphylococcus warneri	ATCC 17917	Skin
Staphylococcus warneri	ATCC 49454	Unknown
Converse bacterial strains		
Escherichia coli	ATCC 8739	Feces
Escherichia coli	ATCC 25922	Clinical isolate
Escherichia coli serotype O157:H7	ATCC 35150	Human feces
Escherichia coli serotype O157:H7	ATCC 700728	Unknown
Proteus mirabilis	ATCC 25933	Human vagina
Salmonella enterica subsp. *indica*	ATCC 43976	Unknown
Salmonella enterica subsp. *enterica* serovar Enteritidis	ATCC 13076	Unknown
Salmonella enterica subsp. *enterica* serovar Enteritidis	ATCC BAA-1045	Raw almonds
Salmonella enterica subsp. enterica serovar Tallahassee	ATCC 12002	Unknown
Salmonella enterica subsp. *enterica* serovar Typhimurium	ATCC 13311	Food poisoning

[a] Strains were grown on 5% SBA plates for approximately 18 h at 37°C.

[b] NRRL = U.S. Department of Agriculture, Agricultural Research Service Northern Regional Research Laboratory Culture Collection (Peoria, IL).

process. Each strain was measured a minimum of three times in the MIT 1000 using independent cultures for analysis.

(**c**) *Clinical isolate performance testing.*—To evaluate the system's ability to identify bacteria from patient samples rather than laboratory strains, clinical isolates were obtained from UP Health System–Marquette on SBA plates. In total, 90 clinical isolates were obtained in a single-blind manner. The identities of the bacterial samples were known by UP Health System–Marquette and unknown to our laboratory. Each SBA plate was labeled with a five-digit identification number. The set of clinical isolates included at least three different *Staphylococcus* species (one strain was not identified to the species level). as well as isolates from 10 other genera. The number of *Staphylococcus* strains provided was unknown upon arrival. Sterile SBA plates were labeled with a corresponding identification number and each isolate was streaked for isolation and cultured for 18 ± 2 h at 37°C. Each of the 90 blind-coded clinical isolates was prepared using the sample preparation from agar culture procedure described above. Each blind-coded clinical isolate was independently measured a minimum of three times in the MIT 1000 using a different colony from the same SBA plate for analysis. After completion of all analyses, results were compared with the known identifications made by UP Health Systems Microbiology Laboratories.

Results and Discussion

Performance Testing: Bacterial Strains Grown on Solid Agar Media

For light-scattering technology to be useful in identifying the genus *Staphylococcus*, the genus *Staphylococcus* Identifier must be able to identify a variety of *Staphylococcus* species and strains and not identify non-*Staphylococcus* strains as *Staphylococcus*. To test the discrimination of the Identifier, 10 *Staphylococcus* strains, including 5 strains of *S. aureus*, 4 strains of *S. epidermidis*, and 1 strain of *S. intermedius*; and 6 non-*Staphylococcus* species, including 3 species of *Streptococcus*, 1 strain of *Micrococcus luteus*, 1 strain of *E. coli*, and 1 strain of *L. monocytogenes*, were analyzed (*see* Table 3). Like *Staphylococcus, Streptococcus pyogenes*, *Streptococcus agalactaie*, *Streptococcus salivarius*, and *M. luteus* are Gram-positive cocci

Table 3. Bacterial strains used to test the performance of the genus *Staphylococcus* Identifier on solid or in liquid media

Organism	Source and strain	Origin
	Inclusive strains	
Staphylococcus aureus subsp. *aureus*[a,b]	ATCC 25923	Clinical isolate
Staphylococcus aureus[a,b]	BEI[c] HI022	Labial abscess
Staphylococcus aureus subsp. *aureus*[a]	ATCC 29213	Wound
Staphylococcus aureus subsp. *aureus*[a,b]	ATCC 6538	Human lesion
Staphylococcus aureus[a]	BEI FN003BN2-C	Nasal colonizer
Staphylococcus epidermidis[a,b]	ATCC 49461	Clinical isolate
Staphylococcus epidermidis[a]	ATCC 49134	Clinical isolate
Staphylococcus epidermidis[a,b]	ATCC 35983	Human blood
Staphylococcus epidermidis[a]	BEI SK135	Human skin
Staphylococcus intermedius[a]	ATCC 29663	Pigeon nares
	Exclusive strains	
Streptococcus pyogenes[a,b]	BEI MGAS 1882	Clinical isolate
Streptococcus agalactiae[a,b]	BEI MNZ933	Human blood
Streptococcus salivarius[a]	BEI SK126	Normal human skin
Micrococcus luteus[a,b]	BEI SK58	Normal human skin
Bacillus subtilis[b]	ATCC 11774	Unknown
Escherichia coli[a,b]	ATCC 29425	Unknown
Listeria monocytogenes[a,b]	ATCC 19115	Human

[a] Strains tested on solid media.

[b] Strains tested in liquid media.

[c] BEI = BEI Resources (Manassas, VA).

(spherical in shape), thereby providing the greatest challenge for the Identifier. *E. coli*, a Gram-negative bacillus, and *L. monocytogenes*, a Gram-positive bacillus, should be less of a challenge for light-scattering technology due to their rod-like shape. Four different types of solid media were used to determine whether the type of media had any effect on the ability of the genus *Staphylococcus* Identifier to accurately identify the strains. The type of growth media could potentially alter the characteristics of the bacteria due to changes in gene expression, which could result in changes in light-scattering patterns.

A summary of the identification results can be found in Figure 9. Each bacterial strain was individually measured a minimum of 10 times in the MIT 1000. When grown on SBA, BHI agar, LB agar, or TSA, the five *S. aureus* strains were successfully identified as the genus *Staphylococcus* by the

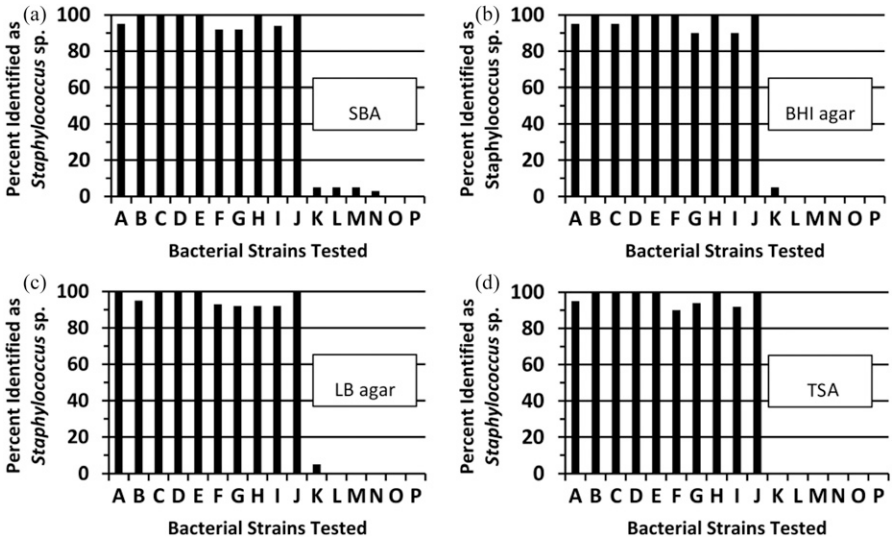

Figure 9. Percent of bacteria measurements identified as a *Staphylococcus* sp. when grown on (a) SBA, (b) BHI agar, (c) LB agar, and (d) TSA. Each strain was measured in the MIT 1000 a minimum of 10 times. Bacterial strains tested are as follows: (A) *S. aureus* ATCC 25923, (B) *S. aureus* HI022, (C) *S. aureus* ATCC 29213, (D) *S. aureus* ATCC 6538, (E) *S. aureus* F003B2NL, (F) *S. epidermidis* ATCC 49461, (G) *S. epidermidis* ATCC 49134, (H) *S. epidermidis* ATCC 35983, (I) *S. epidermidis* SK135, (J) *S. intermedius* ATCC 29663, (K) *S. pyogenes* MGAS1882, (L) *S. agalactiae*, (M) *S. salivarius* SK126, (N) *M. luteus* SK58, (O) *E. coli* ATCC 29425, and (P) *L. monocytogenes* ATCC 19115.

MIT 1000 Identifier 95–100% of the time; the four *S. epidermidis* strains were successfully identified as genus *Staphylococcus* 92–100% of the time; and the one *S. intermedius* strain was successfully identified as genus *Staphylococcus* 100% of the time. These data suggest that the genus *Staphylococcus* can be reliably identified based on the light-scattering properties of the cells. Strain variation between different *S. aureus* isolates had a minimal effect on correct identification. *S. epidermidis* isolates showed the most variability of correct identification. For example, *S. epidermidis* 49461 and 49134 were correctly identified 92% of the time on SBA, whereas *S. epidermidis* 35983 was correctly identified 100% of the time. These data suggest that within certain species of *Staphylococcus*, strain variation has a minimal effect on identification by light scattering. Growth of the strains from the genus *Staphylococcus* on the media used in this study also had no significant effect on their identification by light scattering.

The misidentification rates for the non-*Staphylococcus* bacterial species were also measured. A misidentification in this study was defined as *Streptococcus*, *Micrococcus*, *E. coli*, or *L. monocytogenes* being identified as genus *Staphylococcus* by the MIT 1000. The Gram-positive cocci had low misidentification rates. *S. pyogenes* yielded 5.3, 7.1, 5.3, and 0% misidentification; *S. agalactiae* yielded 6.3, 0, 0, and 0% misidentification; *S. salivarius* yielded 7.1, 0, 0, and 0% misidentification; and *M. luteus* yielded 3.6, 0, 0, and 0% misidentification when grown on SBA, BHI agar, LB agar, and TSA, respectively. *S. pyogenes* was more likely to be misidentified, and misidentification was more likely to occur when Gram-positive cocci were grown on SBA. No misidentifications were observed for *E. coli* and *L. monocytogenes* grown on any of the four media. These data suggest that non-*Staphylococcus* bacterial species, even those that are similar in size and shape, such as *Streptococcus* and *M. luteus*, are rarely misidentified as the genus *Staphylococcus* by light scattering.

Instrument Performance Identifying Bacterial Strains Grown in Liquid Media

If *Staphylococcus* cells grown on solid media can be identified by laser light scattering, then it might be possible to use this technology to identify bacteria grown in liquid culture. To test this question, selected strains from Table 3 were first grown overnight at 37°C on SBA media. One colony of each strain was used to inoculate 2 mL TSB, 2 mL BHI broth, or 2 mL LB broth. The broth tubes were shaken at 200 rpm for 18 ± 2 h at 37°C. Following incubation, each sample was processed as indicated in *Experimental* section. Each sample was measured in the MIT 1000 in triplicate using independent cultures for analysis.

The results of the identification of bacterial cells grown in liquid culture are shown in Figure 10. All six *Staphylococcus* strains were correctly identified 100% percent of the time as the genus *Staphylococcus* regardless of the type of liquid medium tested. All non-*Staphylococcus* strains tested were correctly identified as non-*Staphylococcus* regardless of the liquid medium type. Thus, for the strains tested, the broth cultures resulted in better discrimination of the genus *Staphylococcus* versus non-*Staphylococcus* than solid medium cultures.

Instrument Performance Identifying Staphylococcus Species from Clinical Isolates

Bacteria isolated from infected individuals can vary significantly from laboratory strains of the same species. For example, pathogenic *E. coli* strains that infect people are significantly different from nonpathogenic laboratory strains. Previous studies (33) with *E. coli* have highlighted significant differences in the genomes of laboratory strains and clinical isolates, which may lead to phenotypic changes to the microbe's physical structure. To determine whether the MIT 1000 genus *Staphylococcus* Identifier could specifically identify clinical isolates from the genus *Staphylococcus* and distinguish them from non-*Staphylococcus* isolates, a single-blind study was

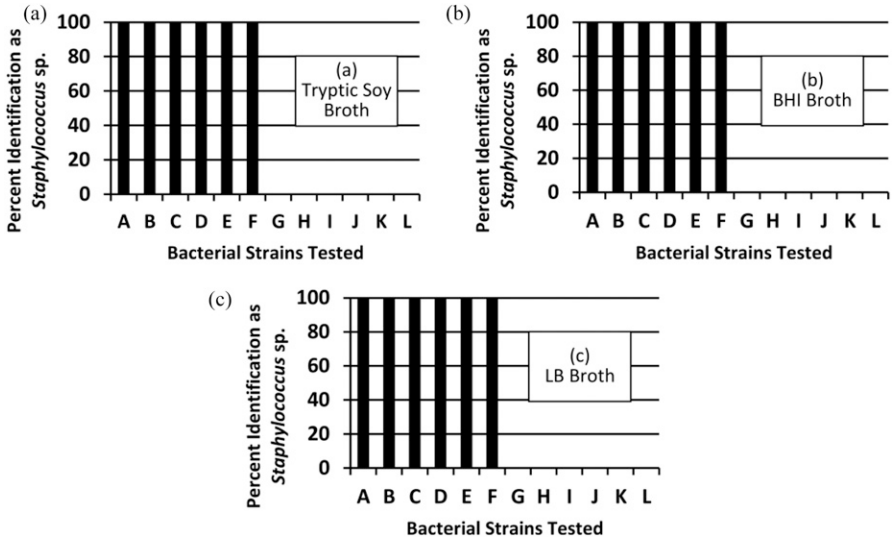

Figure 10. Percent of bacteria measurements identified as a *Staphylococcus* sp. when grown in (a) TSB, (b) BHI broth, and (c) LB broth. Bacterial strains tested are as follows: (A) *S. aureus* ATCC 25923, (B) *S. aureus* HI022, (C) *S. aureus* ATCC 6538, (D) *S. epidermidis* ATCC 49461, (E) *S. epidermidis* ATCC 49134, (F) *S. epidermidis* ATCC 35983, (G) *S. pyogenes* MGAS1882 (H) *S. agalactiae* MNZ933, (I) *M. luteus* SK58, (J) *E. coli* ATCC 29425, (K) *L. monocytogenes* ATCC 19115, and (L) *B. subtilis* ATCC 11774.

performed in collaboration with UP Health Systems–Marquette. UP Health Systems–Marquette provided a random selection of 90 blind-coded bacterial samples isolated from different patients. The isolates were provided on SBA plates and subjected to MIT 1000 identification testing according to the method for solid agar plates. Each hospital isolate was measured in triplicate by the MIT 1000. In all cases, the triplicate measurements for each individual isolate returned the same identification result. The MIT identifications were then compared with the identifications determined by the UP Health Systems–Marquette microbiology laboratory. The results shown in Table 4 indicate that of the 90 bacterial samples provided, the MIT 1000 identified 30 samples as genus *Staphylococcus*. The other 60 hospital isolates included other Gram-positive and -negative bacteria as shown in Table 4. Comparison of the MIT 1000 results with the hospital-determined identification indicated that the MIT 1000 correctly identified 100% of the cultures that were genus *Staphylococcus* and that no misidentifications occurred.

Conclusions

This study demonstrated a proof of concept that a novel laser light-scattering technology could be used to identify bacteria at the genus level by measuring light-scattering patterns off unlabeled cells. Particle size, shape, surface structure, and internal contents can all influence how a particular particle will scatter light. Bacterial cells can be thought of as small particles, and different species of bacteria have specific shapes, sizes, and internal characteristics that cause them to scatter laser light into distinctive patterns. These light-scattering patterns can be analyzed in the MIT 1000 and compared with known light-scattering patterns established for a particular genus or species of bacteria. Our study results demonstrated that light scattering could be used to successfully identify select strains from the genus *Staphylococcus* grown on four commonly used laboratory agar media with over 90% accuracy and distinguish the light-scattering patterns of the genus *Staphylococcus* from morphologically similar strains, such as *Streptococcus* and *Micrococcus*. Liquid culture using three common nonselective broths yielded 100% accuracy in identifying strains from the genus *Staphylococcus* and distinguishing from them non-*Staphylococcus* bacteria. In addition to laboratory strain testing, the data from a single-blind study using clinical isolates demonstrated that the MIT 1000 was highly successful at identifying clinical strains of *S. aureus* from SBA. The data in Figures 9 and 10 and Table 4 demonstrate that the MIT 1000 can accurately identify both laboratory and clinical strains of *Staphylococcus* from solid media and laboratory strains from liquid media. The MIT 1000 light-scattering technology allowed identification of bacteria from an isolated colony or pure liquid culture in less than 5 min. Additionally, the plastic tube, plastic loop, parafilm, water, and reusable sample vials needed to run the test are fairly inexpensive compared with other testing methods. The speed and cost-effective nature of the test may further support its application in industries seeking rapid-identification technology.

Future directions are to further refine the genus *Staphylococcus* Identifier and develop a more specific Identifier for *S. aureus*. A cost-effective method to rapidly identify *S. aureus* from colonies could have valuable use in monitoring food safety. The use of this technology could also have benefits for medical diagnostics and other industries seeking faster bacterial identification.

A current limitation of this technology is that it still requires the growth of colonies on agar plates or in a pure liquid culture, which can take approximately 16–18 h for some bacteria, like *E. coli* or *S. aureus*. In principle, the laser light-scattering technology only needs cells, not colonies, for identification. To reduce the time for bacterial identification, in the future we aim to couple light-scattering technology with immunomagnetic separation (IMS) of bacterial cells. IMS techniques already exist for *S. aureus* and only take a few hours (34, 35) to complete. Essentially this process uses magnetic beads coupled with an antibody that binds to a specific *S. aureus* protein. Anti-protein A antibodies coupled to the beads specifically bind to the protein A on the surface of *S. aureus* cells. After the beads bind *S. aureus* cells, they can be captured in a magnetic field (36) and separated from other microorganisms, cells, or food particles in a liquid matrix. A similar IMS method for *S. aureus* utilizes magnetic beads coupled to mannose-binding lectin that binds to carbohydrates on the surface of *S. aureus* cells (33).

To develop a rapid-identification procedure for *S. aureus*, a food sample, clinical sample, or other liquid matrix could be mixed with anti-protein A beads or mannose-binding lectin beads. A magnetic field could be used to specifically capture *S. aureus* cells. A future goal is to recover the *S. aureus* from the

Table 4. Summary of single-blind clinical study results

Species of clinical isolates[a]	*n*[b]	*X*[c]
Corynebacterium diphtheriae	1	0
Corynebacterium sp.	1	0
Enterobacter cloacae	1	0
Enterococcus faecalis[d,e]	13	0
Enterococcus faecium[d,e]	1	0
Enterococcus sp.[d,e]	2	0
Escherichia coli	14	0
Klebsiella pneumoniae	5	0
Neisseria sp.[e,f]	1	0
Proteus mirabilis	4	0
Providencia rettgeri	1	0
Pseudomonas aeruginosa	2	0
Staphylococcus aureus[d,e]	16	16
Staphylococcus aureus (methicillin-resistant)[d,e]	8	8
Staphylococcus epidermidis[d,e]	4	4
Staphylococcus simulans[d,e]	1	1
Staphylococcus sp. (coagulase-negative)[d,e]	1	1
Streptococcus group A[d,e]	4	0
Streptococcus group B[d,e]	4	0
Streptococcus group C[d,e]	1	0
Streptococcus group D (not *Enterococcus* sp.)[d,e]	1	0
Streptococcus pneumoniae[d,e]	1	0
Viridans streptococci[d,e]	3	0

[a] Genus/species determination was made by the clinical laboratory.

[b] *n* = Number of isolates tested.

[c] *X* = Number of isolates identified as genus *Staphylococcus* by the MIT 1000.

[e] Gram-positive cocci.

[f] Gram-negative cocci.

beads and subject it to identification by laser light scattering. This could potentially reduce the identification time from 16–18 h to less than a typical 8 h work shift.

A critical part of identifying IMS-captured bacteria with laser light scattering would be that these cells would be growing in a liquid culture media. Our results in Figure 10 suggest that MIT 1000's laser light technology can accurately identify *Staphylococcus* cells grown in several nonselective liquid culture broths. Therefore, it should be possible to couple IMS to rapid identification by laser light scattering. Coupling light scattering-based identification to IMS-captured cells remains to be tested, but if successful, the economic and health benefits derived from reduced time to identification would be obvious.

Acknowledgments

We thank Sharon Brunelle Ph.D., AOAC consultant, for editorial support; and Michael Broadway, College of Arts and Sciences at Northern Michigan University, for academic support.

References

(1) Klein, E., Smith, D.L., & Laxminarayan, R. (2007) *Emerg. Infect. Dis.* **13**, 1840–1846. doi:10.3201/eid1312.070629

(2) Bae, E., Ying, D., Kramer, D., Patsekin, V., Rajwa, B., Holdman, C., Sturgis, J., Davisson, V.J., & Robinson, J.P. (2012) *J. Biol. Eng.* **6**. doi:10.1186/1754-1611-6-12

(3) Banada, P.P., Guo, S., Bayraktar, B., Bae, E., Rajwa, B., Robinson, J.P., Hirleman, E.D., & Bhunia, A.K. (2007) *Biosens. Bioelectron.* **22**, 1664–1671. doi:10.1016/j.bios.2006.07.028

(4) Huff, K., Aroonnual, A., Littlejohn, A.E.F., Rajwa, B., Bae, E., Banada, P.P., Patsekin, V., Hirleman, E.D., Robinson, J.P., Richards, G.P., & Bhunia, A.K. (2012) *Microb. Biotechnol.* **5**, 607–620. doi:10.1111/j.1751-7915.2012.00349.x

(5) Singh, A.K., Bettasso, A.M., Bae, E., Rajwa, B., Dundar, M. M., Forster, M.D., Liu, L., Barrett, B., Lovchik, J., Robinson, J.P., Hirleman, E.D., & Bhunia, A.K. (2014) *MBio* **5**. doi:10.1128/mBio.01019-13

(6) Koch, A.L., & Ehrenfeld, E. (1968) *Biochim. Biophys. Acta, Gen. Subj.* **165**, 262–273. doi:10.1016/0304-4165(68)90054-8

(7) Wyatt, P.J. (1968) *Appl. Opt.* **7**, 1879–1896. doi:10.1364/AO.7.001879

(8) Katz, A., Alimova, A., Xu, M., Rudolph, E., Shah, M.K., Savage, H.E., Rosen, R.B., McCormick, S.A., & Alfano, R.R. (2003) *IEEE J. Sel. Top. Quantum Electron.* **9**, 277–287. doi:10.1109/JSTQE.2003.811284

(9) Jo, Y., Jung, J., Kim, M., Park, H., Kang, S., & Park, Y. (2015) *Opt. Express* **23**, 15792–15805. doi:10.1364/OE.23.015792

(10) Chang, Y., Yang, C., Sun, R., Cheng, Y., Kao, W., & Yang, P. (2013) *Sci. Rep.* **3**. 10.1038/srep01863

(11) Konokhova, A.I., Gelash, A.A., Yurkin, M.A., Chernyshev, A.V., & Maltsev, V.P. (2013) *Cytometry A* **83A**, 568–75, https://dx.doi.org/10.1002/cyto.a.22294. doi:10.1002/cyto.a.22294

(12) Michie, D., Spiegelhalter, D.J., & Taylor, C.C. (1994) *Machine Learning, Neural and Statistical Classification*, Ellis Horwood, Upper Saddle River, NJ

(13) Ricardi, J., Haavig, D., Cruz, L., Paoli, G., & Gehring, A. (2010) *J. AOAC Int.* **93**, 249–258, http://pubag.nal.usda.gov/pubag/downloadPDF.xhtml?id=41910&content=PDF

(14) AOAC Research Institute *Performance Tested Method*SM Certificate No. 060901 for the identification of *Listeria* spp.

(15) David, M., & Daum, R. (2010) *Clin. Microbiol. Rev.* **23**, 616–687. doi:10.1128/CMR.00081-09

(16) Patrick, S., & Peterson, M. (2012) *Schaechter's Mechanisms of Microbial Disease*: Lippincott Williams & Wilkins, Philadelphia, PA

(17) Aarestrup, F.M., Larsen, H.D., & Jensen, N.E. (1999) *Vet. Microbiol.* **66**, 165–170. doi:10.1016/S0378-1135(99)00005-X

(18) Brown, D.F.J. (2005) *J. Antimicrob. Chemother.* **56**, 1000–1018. doi:10.1093/jac/dki372

(19) Maree, C.L., Daum, R.S., Boyle-Vavra, S., Matayoshi, K., & Miller, L.G. (2007) *Emerg. Infect. Dis.* **13**, 236–242. doi:10.3201/eid1302.060781

(20) Wang, N., Neilan, A.M., & Klompas, M. (2013) *Infect. Dis. Rep.* **5**. doi:10.4081/idr.2013.e3

(21) Wyatt, P.J., & Jackson, C. (1989) *Limnol. Oceanogr.* **34**, 96–112. doi:10.4319/lo.1989.34.1.0096

(22) Bohren, C.F., & Huffman, D. (1983) *Absorption and Scattering of Light by Small Particles*, John Wiley and Sons, New York, NY

(23) Perry, M.J., & Porter, S.M. (1989) *Limnol. Oceanogr.* **34**, 1727–1738. doi:10.4319/lo.1989.34.8.1727

(24) Balaev, A.E., Dvoretski, K.N., & Doubrovski, V.A.V. (2003) *Proceedings of SPIE 5068, Saratov Fall Meeting 2002: Optical Technologies in Biophysics and Medicine IV* **375**, http://dx.doi.org/ 10.1117/12.518853

(25) Mie, G. (1908) *Ann. Phys.* **330**, 377–445. doi:10.1002/andp.19083300302

(26) MIE Scattering Calculator (2017) Oregon Medical Laser Center, http://omlc.org/calc/mie_calc.html (accessed on 1, March 2017)

(27) Histogram (2003–2013) *NIST/SEMATECH e-Handbook of Statistical Methods*, http://www.itl.nist.gov/div898/handbook/eda/section3/histogra.htm (accessed on 1 March 2017)

(28) Theodoridis, S., & Koutroumbas, K. (2008) *Pattern Recognition*, Academic Press, Burlington, MA

(29) Probability (2016) Wikipedia, The Free Encyclopedia https://en.wikipedia.org/wiki/Probability#Independent_events (accessed on 1 March 2017)

(30) Quality Control Strains (2017) American Type Culture Collection, Manassas, VA, https://www.atcc.org (accessed on 1 March 2017)

(31) Agricultural Research Service Culture Collection (2017) National Center for Agricultural Utilization Research, Peoria, IL, http://nrrl.ncaur.usda.gov (accessed on 1 March 2017)

(32) Culture Collections (2017) National Collection of Type Cultures, http://www.phe-culturecollections.org.uk/collections/nctc.aspx (accessed on 1 March 2017)

(33) Perna, N.T., Plunkett, G., Burland, V., Mau, B., Glasner, J.D., Rose, D.J., Mayhew, G.F., Evans, P.S., Gregor, J., Kirkpatrick, H.A., Pósfai, G., Hackett, J., Klink, S., Boutin, A., Shao, Y., Miller, L., Grotbeck, E.J., Davis, N.W., Lim, A., Dimalanta, E.T., Potamousis, K.D., Apodaca, J., Anantharaman, T.S., Lin, J., Yen, G., Schwartz, D.C., Welch, R.A., & Blattner, F.R. (2001) *Nature* **409**, 529–533. doi:10.1038/35054089

(34) Johne, B., Jarp, J., & Haaheim, L.R. (1989) *J. Clin. Microbiol.* **27**, 1631–1635

(35) Bicart-See, A., Rottman, M., Cartwright, M., Seiler, B., Gamini, N., & Rodas, M. (2016) *PLoS One*. 10.1371/journal.pone.0156287

(36) Gao, J., & Stewart, G.C. (2004) *J. Bacteriol.* **186**, 3738–3748. doi:10.1128/JB.186.12.3738-3748.2004

(37) Ma, X., Lu, J.Q., Brock, R.S., Jacobs, K.M., & Yang, P., & Xin-Hua, H. (2003) *Phys. Med. Biol.* **48**, 4165–4172. doi:10.1088/0031-9155/48/24/013